Using Structural Data to Indicate the Folding Type of Anticlines Examples from the Kurdistan Region, Iraq

Varoujan K. Sissakian[1†] and Lanja H. Abdullah[2]

[1]Department of Petroleum Engineering, Komar University of Science and Technology, Sulaymaniyah 46012, Kurdistan Region – F.R. Iraq

[2]Department of Earth Sciences and Petroleum, College of Science, University of Sulaimani, Sulaimaniyah, Kurdistan Region – F.R. Iraq

***Abstract*—Using seismic data is the most relevant and sound method to indicate the folding type in anticlines. However, when seismic data are not available or not allowed for use, then structural data are recommended to indicate the folding type of any anticline. Such usage is known and considered worldwide with excellent results. We have adopted a sound and published opinion of using structural data to indicate the folding type, and applied the method on three anticlines, namely, Qara Boutaq, Korek, and Mateen. We have selected the three anticlines from three different tectonic zones in the Iraqi Kurdistan Region, which is located in the northern and northeastern parts of Iraq, and forms the northeastern part of the Arabian Plate. The plate has been colliding with the Eurasian Plate since the Late Cretaceous and is still in collision; accordingly, all the existing anticlines are developed. We used satellite images to measure the required structural parameters, including aspect ratio, fold symmetry index, and Mountain Front Sinuosity Index in these anticlines. We also measured the dip amounts along the three anticlines from satellite images, where there are no dip measurements in the geological maps, to indicate the geometrical type of the three anticlines. Part of the interpreted data was checked and confirmed in the field, wherever it was accessible. Accordingly, we indicated the folding type to be Detachment Fold for the Qara Boutaq and Korek anticlines and Fault-bent Fold for the Mateen anticline.**

***Index Terms*—Aspect Ratio, Detachment fold, Fault-bend fold, Fold type, Fold symmetry index.**

I. Introduction

Using structural data when seismic data are not available to indicate the folding type is a well-known method worldwide, and the results are sound (Burberry, Cosgrove and Liu, 2010). Iraqi Kurdistan Region (KRI) occupies the northern and northeastern parts of Iraq, which are located in the northeastern part of the Arabian Plate. Due to the collision of the Arabian and Eurasian plates (Alavi, 2004) (Fig. 1), tens of anticlines are developed.

The majority of the anticlines in the KRI have a NW-SE trend, which is parallel to the Zagros Range; however, the orientation changes to almost E–W west of the latitude 43°30', which is the trend of the Taurus Range (Sissakian and Fouad, 2015). Some of the anticlines are affected by thrust faults, which almost run parallel to the folds. Usually, the southwestern limb is overthrusted by the northeastern limb, and locally even the axis of the anticline is hindered below the thrust fault (Sissakian and Fouad, 2015). Different fold and fault types are developed in the KRI; they are mainly Detachment Folds and Fault-bend (propagated) Folds (Fouad, 2014).

Few studies dealt with the type of folding in the KRI, especially those that depend on Burberry, Cosgrove and Liu (2007 and 2010). Sissakian, et al. (2022) studied two anticlines in the KRI, named Korek and Pirat anticlines, and found that both are detachment folds. Sissakian and Abdullah (2023) studied the Qara Chough anticline and found that it is a detachment fold. Other studies related directly and/or indirectly to the present studies are: Scott Wilkerson, Medwedeff and Marshak (1991) studied the geometry of fault-related folds using a pseudo-three-dimensional approach. Berberian and Qorashi (1989) studied the coseismic fault-related folding during the South Golbaf earthquake in Iran. Champel et al. (2002) conducted a study that dealt with the growth of fault-related folds in Nepal. Mitra (2002) studied faulted detachment folds using geomorphological and structural forms. Zebari and Burberry (2013) used geomorphic criteria to estimate the direction and magnitude of fold propagation. Zebari and Burberry (2015) used geomorphological indices and structural studies for analyzing 4D fold evolution. Khalaj (2015) used geometric and kinematic status to investigate the types of folds. Ahmed (2019) studied the anticlines in the KRI and found that the majority of the anticlines are characterized by double-plunging symmetrical to semi-symmetrical folds. Ghafur, et al. (2019) studied the lateral growth of the Aqra anticline. Thannoun, Fanoosh and Adeeb (2021) used seismic sections in their conducted study to find the structural setting of three anticlines (Kirkuk, Qara Chough, and Bai Hassan).

ARO-The Scientific Journal of Koya University
Vol. XIII, No.2 (2025), Article ID: ARO.12382. 8 pages
DOI: 10.14500/aro.12382
Received: 26 June 2025; Accepted: 04 November 2025
Regular research paper; Published: 08 December 2025
†Corresponding author's e-mail: varoujan.sissakian@komar.ed.iq

http://dx.doi.org/10.14500/aro.12382

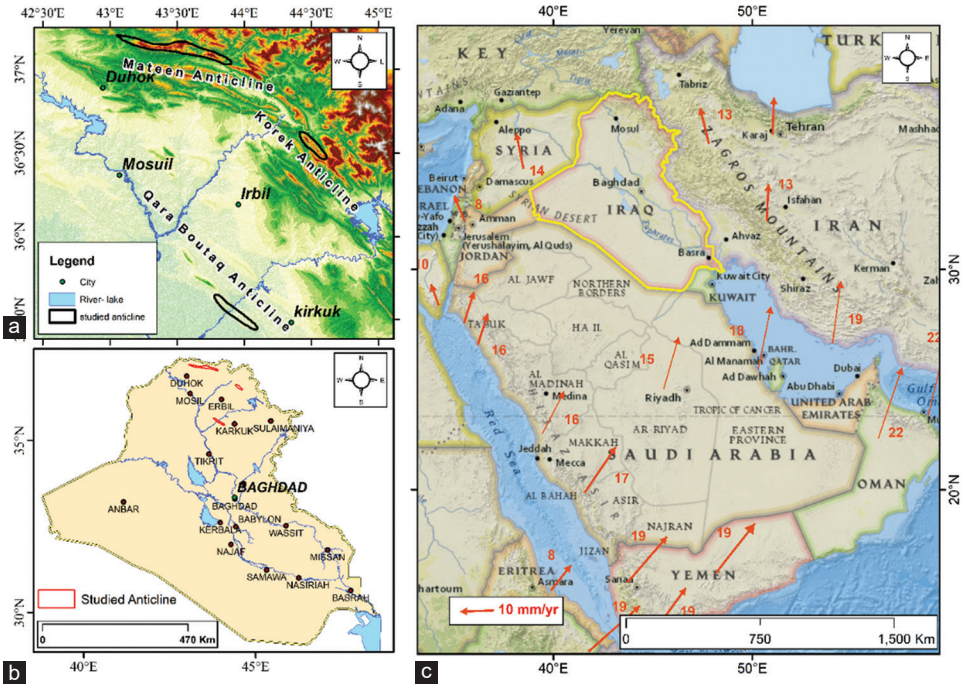

Fig. 1. (a) DEM showing the names of the three studied anticlines, (b) location of the three anticlines in Iraq, (c) Tectonic Map of Saudi Arabia indicating the direction of movements and amount. The international boundaries of Iraq are added by the authors (Modified from Bosworth, 2015).

Ghalandari et al. (2010) studied different anticlines in the Zagros Fold-Thrust Belt in Iran. They concluded that some of the basement faults have major effects on the type of folding and have changed their geometry.

The present study aims to indicate the type of folding in three selected anticlines named Qara Boutaq, Korek, and Mateen. Their locations are shown in Fig. 1. The three anticlines are selected from three different tectonic zones in KRI (Sissakian and Fouad, 2015) to check whether there are some differences in the three tectonic zones, as the type of folding is concerned, which were indicated using structural forms or otherwise. Moreover, this study can be used to indicate the folding type when no seismic data are available, as performed by Burberry, Cosgrove and Liu (2021).

II. Geological Setting

A. Geomorphology

Some common geomorphological units and features are developed along the three studied anticlines (Yacoub, Othman and Kadhim, 2012; Sissakian, et al., 2014) and elsewhere in IKR; among them are: River terraces, alluvial fans, abandoned alluvial fans, anticlinal ridges, hogbacks, and questa, karst forms, landslides, rock falls and very rare creep, water and wind gaps, and different valley types, such as radial, axial, fork-shaped, and inclined (Fig. 2). All these geomorphological features are indications for the tectonic activity and the lateral growth of the majority of the anticlines among which the mentioned features are developed (Burbank and Anderson, 2002; Keller and Pinter, 2002; Ramsey, Walker and Jackson, 2008).

B. Tectonic and Structural Geology

The three anticlines studied, Qara Boutaq, Korek, and Mateen, are located in three different tectonic zones in Iraq (Fouad, 2015). The three tectonic zones and the Zagros Suture Zone are the four main tectonic units (in Iraq) of the Zagros Fold-Thrust Belt, which is a part of the Zagros Foreland Basin. The basin was formed due to the collision of the Arabian and Eurasian plates, with a convergent tectonic boundary, since the Late Cretaceous and is still ongoing (Alavi, 2004; Jassim and Buday, 2006; Sissakian, 2013; Fouad, 2015). The amplitude of the folds and their structural complexity increase in the northern and northeastern parts of the KRI because of their closeness to the collision front. Usually, the south and southwestern limbs are steeper than the northern and northeastern limbs due to the compressional forces and the type of exposed rocks in the anticlines. Moreover, in some anticlines, the northern and northeastern limbs are thrusted over the southern and southeastern limbs, causing the disappearance of part of the overthrusted limb, and locally even the anticlinal axis is covered either partly or totally; accordingly, an axial valley is developed along the thrust fault, especially when soft and/or weak rocks are exposed in the core of the anticline. However, rarely, the southeastern and southern limbs are steeper and even overturned, but none of the northern and northeastern limbs are overturned. Some of the anticlines show many domes, while others exhibit en-echelon plunges with adjacent anticlines (Sissakian and Fouad, 2015).

The geology of the studied anticlines is described briefly; hereinafter.

- Qara Boutaq anticline is developed in the Low-Folded Zone (Fouad, 2015), it consists of two domes: A small

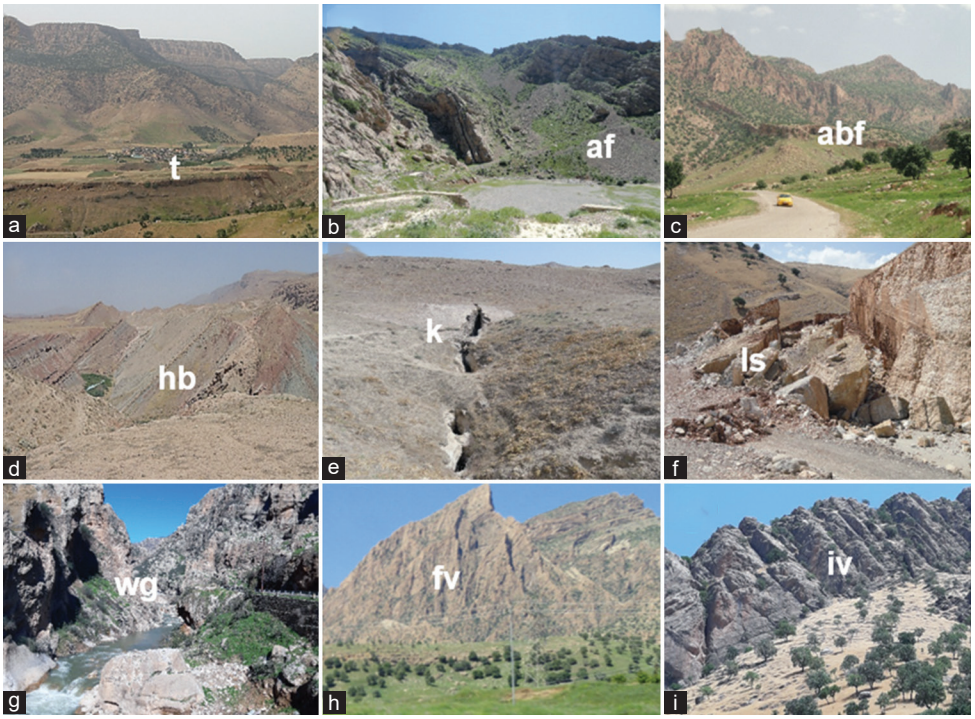

Fig. 2. Different geomorphological features recognized in the Iraqi Kurdistan Region. (a) River terraces (t) along the Rawandouz River near Korek Mountain, (b) Active alluvial fan (af) along the Pera Magroon anticline, (c) Abandoned alluvial fan (abf) along Surdash anticline, (d) Hogback and Questa (hb) along Aj Dagh anticlines, (e) Longitudinal karst (k) along Aj Dagh anticline, (f) Landslide (ls) along Surdash anticline, (g) Water gap along Peris anticline, (h) Anticlinal ridge with fork-shaped valleys (fv) along Surdash anticline, and (i) Inclined valleys (iv) along Surdash anticline.

northwestern dome and a large southeastern dome; their lengths are 5 km and 35 km, respectively. Both domes are double plunging with a steep southwestern limb, with an average dip of 34°; whereas the average dip of the northeastern limb is 27° (Sissakian, 1995).

- Korek anticline is developed in the High-Folded Zone (Fouad, 2015). Its length is 27 km and width of about 7.10 km; trending NW-SE and almost symmetrical limbs where the northeastern and southwestern limbs dip 41° and 37°, respectively. The anticline consists of three domes, and the northwestern plunge is truncated by a reverse fault (Sissakian and Fouad, 2014).
- Mateen anticline is developed in the Imbricate Zone (Fouad, 2015). The length and width of the anticline are 76 km and 11.3 km, respectively, with a trend of approximately E–W. It is an asymmetrical anticline with a steeper northern limb with an average dip of 29°, whereas the average dip of the southern limb is 17°. The western plunge is truncated by three strike-slip faults, and the axis, further westward, is covered by the main Zagros Thrust Fault (Sissakian and Fouad, 2014).

C. Stratigraphy

Fig. 3. shows the formations that are exposed in the three studied anticlines. However, some of the presented formations are either exposed in the three anticlines or in subsurface sections. This presentation will elucidate the possibility of some subsurface formations, which may act as a detachment horizon in some folds. Moreover, the Adaiyah, Alan, and Gotnia formations of the Jurassic age may also act as a detachment horizon, although not presented in Fig. 3, because we don't have sound data to present them in the generalized columnar stratigraphic section. The mentioned three anticlines may act as detachment horizons because they include gypsum and anhydrite layers. Even in Iran, they are considered as detachment layers (Ghanadian, et al., 2017).

III. Used Data and Methodology

To conduct this research, we used different geological and topographical maps of the 1:100000 scale, named Makhmour, Rawandouz, and Amadiya (GEOSURV, 1997). Satellite images of Sentinel-2 L2A type were also used to indicate and measure some geomorphological and structural features and parameters.

The main opinion of the present work is based on the opinion of Burberry, Cosgrove and Liu (2010). To calculate the required parameters, aspect ratio (AR) and fold symmetry index (FSI), we have measured different structural features (Fig. 4) at each anticline to elucidate the folding type.

We also have calculated and indicated different structural aspects of the studied folds using the mentioned topographic and geological maps, and satellite images; these are: (1) Length, (2) Hinge length, (3) Width, (4) Width of the forelimb, (5) AR, (6) FSI, and (7) Mountain Front Sinuosity Index (Smf) (Table I). We have calculated the following aspects, using different equations, as shown hereinafter.

http://dx.doi.org/10.14500/aro.12382

Era	Period	Epoch		Formations/ Sediments	General Lithology (Thickness, m)
CENOZOIC	QUATERNARY	Holocene		Floodplain, Valley fill	Silt, clay, and sand with rare pebbles (1-3)
		Pleistocene		Slope, River terraces, Alluvial fans	Rock fragments, fairly cemented (1-8) Pebbles and/ or rock fragments cemented (2-10)
	NEOGENE	Pliocene		Bai Hassan	Conglomerate and red-brown claystone (≥ 300)
		Miocene	U	Mukdadiya, Injana	Sandstone, siltstone and claystone (≥ 600)
			M	Fatha	Marl, gypsum, limestone/ red fine clastics (~250)
			L	Euphrates, Serikagni, Jeribe	Mainly limestone and dolostone (100- 150)
	PALEOGENE	Oligocene	U	Azkand, Anah, Ibrahim	Mainly limestone (Altogether 120- 230)
			M	Tarjil, Baba, Bajwan	
			L	Palani, Shurau, Sheikh Alas	
		Eocene	U	Pila Spi, Jaddala, Avanah	Mainly limestone and dolostone (80- 190)/ (40- 45)/ (35 – 150)
			M	Gercus	Red fine clastics (300 – 850)
			L		
		Paleocene	U	Khurmala, Sinjar	Mainly limestone (10- 85)/ (45-65)
			L	Kolosh/ Aaliji	Black fine clastics/ Marl, limestone, shale (300 – 400)/ (200-350)
MESOZOIC	Cretaceous		U	Tanjero/Shiranish/ Bekhme	Clastics/ Marly limestone/ Limestone (300-650)/ (250-650)/ (85-320)
			L	Kometan, Gulneri, Dokan, Qamchuqa, Balambo, Sarmord	Mainly carbonates with rare marl and shale (140-300)/ (few meters, each)/ (300- 650)/ (300- 650)/ (300- 650)
	Jurassic		U	Chia Gara, Barsarin, Naokelekan	Mainly carbonates (90-230)/ (14)/ (16) (150-300) (200-250)/ (300-400)
			M	Sargelu	
			L	Sehkaniyan, Sarki	
	Triassic		U	Baluti/ Kurra Chine	Shale/ Limestone (35- 42)/ (800-840)
			M	Geli Khana/ Bedu/ Mirga Mir	Black dolostone (550-575)/ (55-65)/ (550-520)
			L		

Fig. 3. Generalized columnar stratigraphic section of the studied area. The colors of the stratigraphic time units are from ICS (2022). Data are from Sissakian and Fouad (2015).

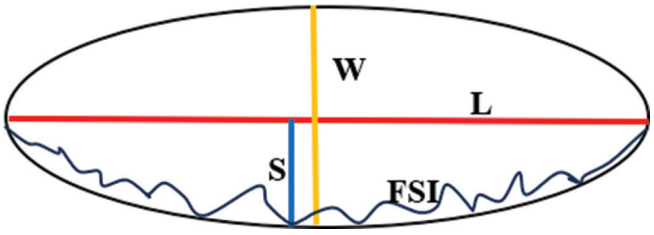

Fig. 4. Diagrammatic presentation of the measured parameters of the studied three anticlines. W: Width, L: Length, S: Width of the fore limb, and FSI: Length of the mountain front (Modified from Burberry, Cosgrove and Liu, 2010).

AR is calculated according to Burberry, Cosgrove and Liu (2010)

$AR = L/E$ (Fig. 3) (1)

Where: L and W are the length and width of the fold, respectively

FSI is calculated according to Burberry, Cosgrove and Liu (2010)

$FSI = S/(W/2)$ (Fig. 3) (2)

Smf is calculated according to Bull and McFaden "(1997)

$Smf = FSI/L$ (Fig. 3) (3)

Where: FSI is the length of the mountain front along the foot of the mountain at the pronounced break in slope, and L is the straight-line length of the mountain front.

We also calculated the dip amount along both limbs and plunges of the three anticlines (Tables II and III) from field observations or geological maps. However, when no dip measurements were available from the used geological maps or the areas were not accessible, we used satellite images to calculate dip measurements. A clear bedding plane was selected; usually, limestone and/or dolostone providing

TABLE I
THE MAIN CALCULATED PARAMETERS WITHIN THE THREE STUDIED ANTICLINES

Anticline name	Length (km)		W (km)	S (km)	FS (km)	AR	FSI	Smf (FFI)	Tectonic zone	Fold type
	Normal (L)	Hinge (Hi)								
Qara Boutaq	37.9	38.11	8.68	3.17	40.9	8.11	0.90	1.08	LF	DF
Korek	27.3	27.97	7.10	3.00	28.9	3.85	1.07	1.06	HF	DF
Mateen	76.3	77.60	11.3	5.12	82.3	6.75	0.99	1.07	Im	FBF

Abbreviations: DF: Detachment fold, FBF: Fault-bend fold. Tectonic zones: LF: Low folded, HF: High folded, and Im: Imbricate

that the measurements will be conducted on the top of the same bedding plane; however, a few differences on the top of the selected bedding plane will not cause a considerable error in the dip measurements, which were calculated using equation (4):

$$Tan\ Ø = H/D \quad (4)$$

Where: H is the height difference between the top and bottom points along a certain bedding plane, which was chosen to calculate the dip amount (Points A and B, Fig. 5)

D is the distance between A and B (Fig. 5) (Measured from the satellite image) Ø is the dip amount.

Totally, at 68 locations (field observations, existing dips on geological maps, and satellite images), the dip amounts were measured (Table II). The measured dips in the field, from geological maps, and from satellite images are 20, 17, and 31 measurements, respectively (Table II). We also compared some of the dip measurements from the satellite images and in the field (the same location) and found that the difference was ± 3 degrees. The average dips of both limbs, plunges, and the orientation of the axial surfaces of the three studied anticlines are presented in Table III.

We couldn't construct sound cross sections in the three studied anticlines because of the lack of seismic and well data. Without such relevant data, the constructed cross sections will not be sound enough to determine the folding type; however, the construction of cross sections based on surface outcrops and dip measurements will not serve to find the folding type.

IV. Results

The results of all performed measurements and calculations of structural features (apart from dip measurements) are presented in Table I. The achieved data from the calculation of AR and FSI of the three anticlines are plotted versus the hinge length of the three anticlines (Fig. 6), which represent the acquired three main folding types by Burberry, Cosgrove and Liu (2010). Accordingly, the folding types of the three studied anticlines were indicated (Fig. 6 and Table I).

The folding type of the studied three anticlines, as indicated by the relation of the AR versus the Hinge length (Fig. 6a), is a Detachment Fold for the Qara Boutaq and Korek anticlines, whereas the Mateen anticline is a Fault-bend Fold. However, when considering FSI versus the Hinge length (Fig. 6b), the Qara Boutaq and Korek anticlines are closer to the Detachment Fold type, whereas the Mateen anticline is closer to the Fault-bend Fold type.

Fig. 5. A chosen bedding plane in the Korek anticline to measure the dip amount.

The geometrical types of the three anticlines based on the classification of Fleuty (1964) are presented in Fig. 7. From Fig. 7, it is clear that the Qara Boutaq anticline is moderately inclined with an almost Horizontal plunge. The Korek anticline is moderately inclined with a Gentle plunge. Whereas the Mateen anticline is steeply inclined with almost a Horizontal plunge.

V. Discussion

Seismic sections and large-scale, detailed geological maps are the best data to indicate the type of folding of any anticline. However, seismic sections are not always available, and even so, they are considered top confidential in Iraq; therefore, they cannot be obtained and used for such interpretations. Besides, large-scale geological maps are also not available in Iraq for publication. Therefore, we indicated the folding type of the studied anticlines based on Burberry, Cosgrove and Liu (2010).

The studied anticlines have shown that the folding types are Detachment Fold for the Qara Boutaq and Korek anticlines, whereas the Mateen anticline is a Fault-bend fold (Fig. 6). However, it can be seen in Fig. 6b that when considering the FSI, the three anticlines are not within the presented three domains, but still, we have considered the nearest domain in assigning the folding type. This is attributed to the measured length of the FSI, which depends on the accuracy of the satellite images used.

The Qara Boutaq and Korek anticlines are found to be Detachment Folds. For the Qara Boutaq anticline, the detachment layer is the anhydrite beds within the Gotnia Formation, which is about 200 m and it is of the Upper Jurassic age (Van Bellen, et al., 1959). The Gotnia Formation is not exposed in the anticline, but is encountered in drilled oil wells in the vicinity (IPC, 1963). According to Jassim and

http://dx.doi.org/10.14500/aro.12382

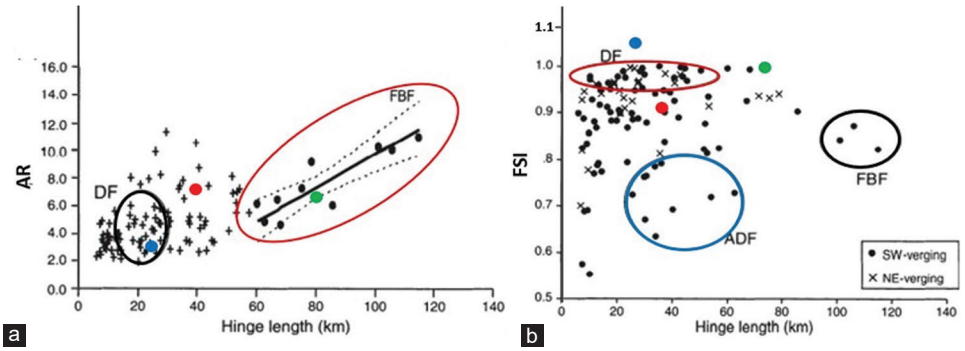

Fig. 6. Fold types based on Burberry, Cosgrove and Liu (2010), (a) aspect ratio, (b) fold symmetry index. The red, blue, and green dots represent the Qara Boutaq, Korek, and Mateen anticlines, respectively. DF: Detachment fold, ADF: Asymmetric detachment fold, and FBF: Fault-bend folds.

TABLE II
Measured Dip Amounts Along Qara Boutaq, Korek, and Mateen Anticlines

Qara Boutaq anticline						Korek anticline						Mateen anticline					
No.	Slope (m)	Height (m)	tan Ø	Dip angle (○)	Location	No.	Slope (m)	Height (m)	tan Ø	Dip angle (○)	Location	No.	Slope (m)	Height (m)	tan Ø	Dip Angle (○)	location
1	2460	886	0.36	20	NW	1	2460	886	0.36	20	NW plunge	1	738	123	0.17	9	NW
2	504	607	1.20	50	plunge	2	2453	736	0.30	17		2	540	88	0.16	9	plunge
3	195	135	0.69	35		3	636	225	0.35	19		3	266	50	0.19	11	
4	302	30	0.11	6	SE plunge	The SE plunge is obscured, it is					SE plunge	4	573	70	0.12	7	SE
5	263	51	0.19	11		truncated by many small thrust faults						5	542	86	0.16	9	plunge
6	300	31	0.11	6								6	515	91	0.18	10	
7	244	138	0.57	30	SW limb	4	901	469	0.52	28	SW limb	7	476	101	0.21	12	SW limb
8	73	64	0.88	41		5	988	503	0.51	27		8	308	33	0.11	6	
9	195	135	0.69	35		6	1321	700	0.53	28		9	219	102	0.47	26	
10	450	312	0.70	35		7	631	205	0.32	18		10	176	92	0.52	28	
11	308	333	1.08	43		8	703	378	0.54	28		11	181	50	0.28	15	
12	244	138	0.57	30		9	102	203	1.99	63		12	192	58	0.30	17	
13	74	65	0.88	42		10	158	312	1.97	63		13	221	106	0.48	26	
14	145	135	0.93	43		14	324	718	2.22	76		14	509	141	0.28	15	
15	447	310	0.70	35		11	638	226	0.35	20		15	168	38	0.23	13	
16	76	67	0.88	41		12	888	214	0.24	14		16	264	49	0.19	11	
17	84	47	0.56	30	NE limb	13	749	333	0.44	24	NE limb	17	74	65	0.88	41	NE limb
18	303	153	0.50	27		14	235	133	0.57	30		18	145	135	0.93	43	
19	63	27	0.43	23		15	204	100	0.49	26		19	244	138	0.57	29	
20	81	44	0.56	30		16	204	157	0.77	38		20	92	41	0.45	24	
21	300	150	0.50	27		17	197	136	0.69	35		21	84	47	0.56	29	
22	63	27	0.43	23		18	455	317	0.70	35		22	303	153	0.50	27	
23	60	26	0.42	23		19	40	550	13.75	85		23	63	27	0.43	23	
24	79	42	0.55	30		20	348	534	1.53	67		24	73	21	0.29	16	
Dip measurements			From the field (20 measurements)						From geological maps (17 measurements)						From satellite images (31 measurements)		

TABLE III
The Averages of Different Measured Dip Amounts

Anticline	Dip average (○)			
	NE limb	SW limb	Plunge	Axial surface
Qara Boutaq	27	34	9	60
Korek	41	37	21	51
Mateen	29	17	9	67

Buday (2006), the formation can be found as lenses within the Upper Jurassic sequence of the Foothill Zone (Low-Folded Zone). Whereas for the Korek anticline, the detachment layer is the Mirga Mir Formation (Lower Triassic), it is about 200 m thick and consists of "thin-bedded, grey and yellow, marly limestones and shales with slump beds and recrystallization breccias; oolitic limestones at the base, with wisps of sandstone" (Van Bellen, et al., 1959). Moreover, the Baluti Formation may also act as a detachment layer because it includes anhydrite (Bellen, et al, 1959 and Mohialdeen, et al., 2022). The Mirga Mir and Baluit formations are not exposed in the anticline, but northwestward and northward, the formation is exposed (Sissakian and Fouad, 2015), which means the formation exists in the subsurface section of the Korek anticline. However, Omar and Othman (2018) measured the depth to the detachment to be in a range of (2.1–3.6) km. These depths are estimated to be under the Qamchuqa Formation, which coincides with the Ora

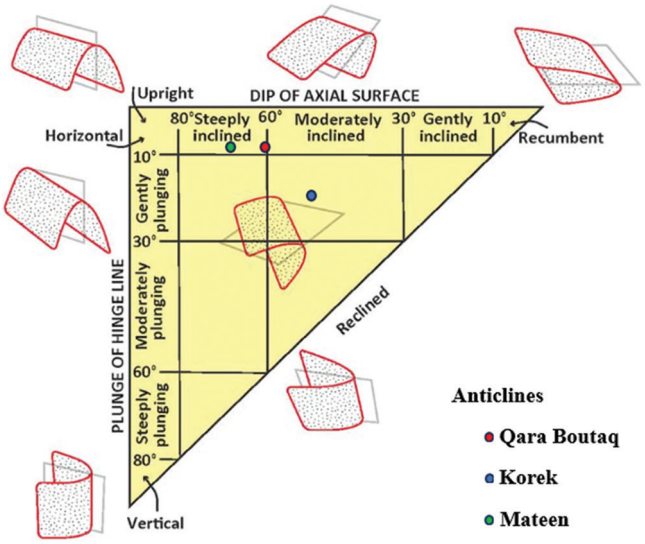

Fig. 7. Fleuty (1964) classification of anticlines showing the geometrical shapes of the three studied anticlines.

Formation of the Upper Paleozoic age. The formation consists mainly of black shale, which can work as a detachment layer. Moreover, the Adaiyah, Alan, and Gotnia formations, which consist mainly of anhydrite and are 90 m, 87 m, and 216 m, respectively (Jassim and Buday, 2006), can work as detachment surfaces. Due to the lack of seismic and oil well data, we cannot determine which of the mentioned formations has the effect of a detachment in the Qara Boutaq and Korek anticlines.

We couldn't detect any difference in the accuracy of identifying the folding type in the three anticlines, which are developed within three tectonic zones of Iraq. Therefore, the opinion of Burberry, Cosgrove and Liu (2010) can be used in any tectonic zone in Iraq.

According to Fleuty's (1964) classification of fold geometry, the Qara Boutaq and Korek anticlines are moderately inclined, whereas the Mateen anticline is steeply inclined. For the plunge form, the Qara Boutaq and Mateen anticlines have an almost Horizontal plunge, whereas the Korek anticline has a Gentle plunge. For the inclination, the Mateen anticline is steeply inclined; this is attributed to its location in the Imbricate Zone (Sissakian and Fouad, 2015), which has received more compressional forces because of its proximity to the collision zone between the Arabian and Eurasian plates (Fouad, 2015). The Qara Boutaq and Korek anticlines showed Moderate inclination, although they are located in the Low-Folded and High-Folded zones, respectively. This is attributed to intensely faulted limbs of the Korek anticline, which hindered the true dip amounts of both limbs, whereas in the Qara Boutaq anticline, the thick calcrete deposits hindered the true dip amounts.

VI. Conclusion

To elucidate the folding type of the three studied anticlines, the AR and FSI were calculated after measuring different structural parameters. The ARs of the three anticlines were found to be 8.11, 3.85, and 6.75, respectively, whereas the Fold Symmetry indices were found to be 0.90, 1.07, and 0.99, respectively. Accordingly, the folding type was found to be a Detachment Fold for the Qara Boutaq and the Korek anticlines, with the Gotnia, Mirga Mir, and Baluti formations being the detachment horizon, respectively. Whereas the Mateen anticline is a Fault-bend Fold. According to the Fluety Classification of folds, the Qara Boutaq and Mateen anticlines have an almost Horizontal plunge, whereas the Korek anticline has a Gentle plunge. For the inclination, the Mateen anticline is steeply inclined; whereas the Qara Boutaq and Korek anticlines showed Moderate inclination.

References

Ahmed, S.H., 2019. Designation and study of anticlines-Kurdistan Region-NE Iraq. *Journal of Physics, Conference Series*, 1294, p. 082001.

Alavi, M., 2004. Regional stratigraphy of the Zagros fold-thrust belt of Iran and its proforeland evolution. *American Journal of Science*, 304, pp. 1-20.

Bellen, R.C. van, Dunnington, H.V., Wetzel, R. and Morton, D., 1959. *Lexique Stratigraphic International*. Asie, Fasc. 10a, Iraq, Paris.

Berberian, M., and Qorashi, M., 1989. Coseismic fault-related folding during the South Golbaf earthquake of November 20, 1989, in southeast Iran. *Geology*, 22, pp. 531-534.

Bosworth, W., 2015. *Geological Evolution of the Red Sea: Historical Background, Review, and Synthesis*. Springer, Berlin.

Bull, W.B., and McFadden, L.D., 1977. Tectonic geomorphology north and south of the Garlock fault, California. *Geomorphology of Arid Regions*. State University of New York, Binghamton, pp. 115-138.

Burbank, D.W., and Anderson, R.S., 2001. Tectonic Geomorphology. 2nd ed. A John Wiley and Sons, Ltd., p. 274.

Burberry, C.M., Cosgrove, J.W., and Liu, J.G., 2007. Stream network characteristics used to infer the distribution of fold types in the Zagros Simply Folded Belt, Iran. *Journal of Maps*, 3, pp. 32-45.

Burberry, C.M., Cosgrove, J.W., and Liu, J.G., 2010. A study of fold characteristics and deformation style using the evolution of the land surface: Zagros Simply Folded Belt, Iran. *Geological Society Special Publication*, 330, pp. 139-154.

Champel, B., Van der Beek, P., Mugnier, J.L., and Pascale Leturmy, L., 2002. Growth and lateral propagation of fault-related folds in the Siwaliks of western Nepal: Rates, mechanisms, and geomorphic signature. *Journal of Geophysical Research*, 107(B6), pp. ETG 2-1-ETG 2-18.

Fleuty, M.J., 1964. The description of folds. *Proceedings of the Geologists/ Association*, 75, pp. 461-492.

Fouad, S.F., 2014. Western zagros fold - thrust belt, part II : The high folded zone. *Iraqi Bulletin of Geology and Mining*, Special issue(6), pp. 53-71.

Fouad, S.F., 2015. Tectonic map of Iraq, scale 1: 1000 000. 3rd ed. *Iraqi Bulletin of Geology and Mining*, 11, pp. 1-7.

GEOSURV (Iraq Geological Survey, Archive), 1997. *Unpublished Geological Maps of Iraq, Scale 1:100000, Baghdad*. Iraq Geological Survey, Archive, Iraq.

Ghafur, A.A., Sissakian, V.K, Abdulhaq, H.A., and OmAr, H.O., 2019. Aqra anticline: A growing structure in the Iraqi Kurdistan Region. *ARO-The Scientific Journal of Koya University*, 7(2), pp. 27-33.

Ghanadian, M., Faghih, A., Fard, I.A., Grasemann, B., Soleimany, B., and Maleki, M., 2017. Tectonic constraints for hydrocarbon targets in the Dezful Embayment, Zagros Fold and Thrust Belt, SW Iran. *Journal of Petroleum Science and Engineering*, 157, pp. 1220-1228.

Ghlandari, S., Maleki, Z., Arian, M., Solgi, A., and Aleali, M., 2023. Basement faults effect on the folding style: A case study from Hendurabi Fault, Zagros, Iran. *Geotectonics*, 57(4), pp. 513-523.

ICS (International Commission on Stratigraphy), 2022. *International Chronostratigraphic Chart*. Internet Data. Available from: https://stratigraphy.org/icschart/chronostratchart2022-10.pdf [Last accessed on 2023 Nov 10].

IPC., 1963. *Geological and Production Data. Iraq Geological Survey Library*, Unpublished Report. No. 130.

Jassim, S.Z., and Buday, T., 2006. In: Jassim, S.Z., and Goff, J., Eds. *Geology of Iraq*. Dolin, Hlavni, Prague and Moravian Museum, Brno, Czech Republic.

Keller, E.A., and Pinter, N., 2002. Active Tectonics. 2nd ed. Prentice Hall, Upper Saddle River, New Jersy, p. 362.

Khalaj, M., 2015. Analysis of Fault-Related Folding in South of Birjand. *Open Journal of Geology*, 5, pp. 394-398.

Mitra, S., 2002. Structural models of faulted detachment folds. *American Association of Petroleum Geologist Bulletin*, 86, pp. 673-1694.

Mohialdeen, I.M.J., Fatah, S.S., Abdula, R.A., Hakimi, M.H., Abdullah, W.H., Khanaqa, P.A., and Lunn, G.A., 2022. Stratigraphic correlation and source rock characteristics of the Baluti Formation from selected wells in the Zagros fold belt, Kurdistan Region, Northern Iraq. *Journal of Petroleum Geology*, 45(1), pp. 29-56.

Omar, A.A., and Othman, A.T., 2018. Morpho-Structural Study of the Korek Anticline, Zagros Fold-Thrust Belt, Kurdistan of Iraq. *Geotectonic*s, 52(3), pp. 382-400

Ramsey, L.A., Walker, R.T., and Jackson, J., 2008. Fold evolution and drainage development in the Zagros mountains of Fars Province, SE Iran, *Basin Research*, 20, pp. 23-48.

Scott Wilkerson, M., Medwedeff, D.A., and Marshak, S., 1991. Geometrical modeling of fault-related folds: A pseudo-three-dimensional approach. *Journal of Structural Geology*, 13, pp. 801-812.

Sissakian, V.K., 1995. *Geological Map of Kirkuk Quadrangle, Scale 1: 250000*. Iraq Geological Survey Publications, Baghdad, Iraq.

Sissakian, V.K., 2013. Geological evolution of the Iraqi Mesopotamia Foredeep, inner platform, and near surroundings of the Arabian Plate. *Journal of Asian Earth Sciences*, 72, pp. 152-163.

Sissakian, V.K., and Abdullah, L.H., 2023. Deducing Folding Form in the Qara Chough South Anticline by Using Structural and Geomorphological Indications in Central Part of Iraq. *Passer*, 5(2), pp. 330-334.

Sissakian, V.K., and Fouad, S.F., 2014. *Geological Map of Erbil and Mahabd Quadrangles, Scale 1: 250000*. 2nd ed. Iraq Geological Survey Publications, Baghdad, Iraq.

Sissakian, V.K., and Fouad, S.F., 2015. *Geological Map of Iraq, Scale 1: 1000 000*. 4th editon. 2012. *Iraqi Bulletin of Geology and Mining*, 11(1), pp. 9-18.

Sissakian, V.K., Gahfur, A.A., Omer, H.O., and Abdulhaq, H.A., 2022. Structural development of the Korek and Pirat anticlines, Iraqi Kurdistan Region. A tectonic-geomorphological study. *Results Geophysical Sciences*, 12, p. 100047.

Sissakian, V.K., Kadhim, T.H., and Abdul Jab'bar, M.F., 2014. Geomorphology of the high folded zone. *Iraqi Bulletin of Geology and Mining*, Special issue(6), pp. 7- 51.

Thannoun, R.G., Fanoosh, S.A., and Adeeb, H.G.M., 2021. Integration of satellite data processing with seismic sections for tectonic interpretation and modeling for the breaks and omissions of continuous stratigraphic units. *International Review of Applied Sciences and Engineering*, 12, pp. 4-43.

Van Bellen, D., Dunnington, R.C., Wetzel, H.V., and Morton, R., 1050. *Lexique Stratigraphique International, Asie, Fasc*. 10a, Iraq, Paris, Centre. National de Ja Recherche Scientifique.

Yacoub, S.Y., Othman, A.A., and Kadhim, T.H., 2012. Geomorphology of the Low Folded Zone. *Iraqi Bulletin of Geology and Mining*, Special issue(5), pp. 7-37.

Zebari, M., and Burberry, C.M., 2013. *Geometry and Evolution of Fold Structures within the high Folded Zone Zagros Fold-Thrust Belt*, *Kurdistan Region, Iraq*. In: Dissertations and Theses in Earth and Atmospheric Sciences, p. 100.

Zebari, M., and Burberry, C.M., 2015. 4-D evolution of anticlines and implications for hydrocarbon exploration within the Zagros Fold-Thrust Belt, Kurdistan Region, Iraq. *GeoArabia*, 20, pp. 161-188.